Central diabetes insipidus associated with impaired renal aquaporin-1 expression in mice lacking liver X receptor β

Chiara Gabbi[a,b], Xiaomu Kong[c,1], Hitoshi Suzuki[b,1], Hyun-Jin Kim[b,1], Min Gao[c], Xiao Jia[c], Hideo Ohnishi[d], Yoichi Ueta[e], Margaret Warner[b], Youfei Guan[c], and Jan-Åke Gustafsson[a,b,2]

[a]Department of Biosciences and Nutrition, Karolinska Institutet, S-141 86 Novum, Sweden; [b]Center for Nuclear Receptors and Cell Signaling, University of Houston, Houston, TX 77204; [c]Department of Physiology and Pathophysiology, Key Laboratory of Cardiovascular Sciences, Peking University Health Science Center, Beijing 100191, China; and Departments of [d]Orthopedics and [e]Physiology, School of Medicine, University of Occupational and Environmental Health, Kitakyushu 8078555, Japan

Contributed by Jan-Åke Gustafsson, January 12, 2012 (sent for review December 31, 2011)

The present study demonstrates a key role for the oxysterol receptor liver X receptor β (LXRβ) in the etiology of diabetes insipidus (DI). Given free access to water, LXRβ$^{-/-}$ but not LXRα$^{-/-}$ mice exhibited polyuria (abnormal daily excretion of highly diluted urine) and polydipsia (increased water intake), both features of diabetes insipidus. LXRβ$^{-/-}$ mice responded to 24-h dehydration with a decreased urine volume and increased urine osmolality. To determine whether the DI was of central or nephrogenic origin, we examined the responsiveness of the kidney to arginine vasopressin (AVP). An i.p. injection of AVP to LXRβ$^{-/-}$ mice revealed a partial kidney response: There was no effect on urine volume, but there was a significant increase of urine osmolality, suggesting that DI may be caused by a defect in central production of AVP. In the brain of WT mice LXRβ was expressed in the nuclei of magnocellular neurons in the supraoptic and paraventricular nuclei of the hypothalamus. In LXRβ$^{-/-}$ mice the expression of AVP was markedly decreased in the magnocellular neurons as well as in urine collected over a 24-h period. The persistent high urine volume after AVP administration was traced to a reduction in aquaporin-1 expression in the kidney of LXRβ$^{-/-}$ mice. The LXR agonist (GW3965) in WT mice elicited an increase in urine osmolality, suggesting that LXRβ is a key receptor in controlling water balance with targets in both the brain and kidney, and it could be a therapeutic target in disorders of water balance.

cholesterol | oxysterols | hormones | pituitary

Diabetes insipidus (DI) is a clinical condition characterized by polyuria (an abnormally high excretion of diluted urine) and by polydipsia (increased thirst and fluid intake) (1). Four subtypes of DI are defined according to etiology: (*i*) central or neurohypophyseal, caused by an inadequate release of the antidiuretic hormone, arginine vasopressin (AVP); (*ii*) nephrogenic, caused by a renal resistance to the action of AVP by a defect either in the AVP receptor (AVPR2) or in the water channel aquaporin-2 (AQP-2); (*iii*) gestational, caused by increased metabolism of vasopressin by vasopressinase produced by the placenta; and (*iv*) polydipsic, induced primarily by high water intake with consequent suppression of vasopressin release (1).

AVP is a nonapeptide produced by magnocellular neurons located in the supraoptic (SON) and paraventricular (PVN) nuclei of the hypothalamus (2). After axonal transport to the posterior pituitary, AVP is stored in vesicles and released in response to an increase in plasma osmotic pressure and sodium concentration (3).

In the kidney, AVP exerts its action by binding to AVPR2. In response to AVP there is an increased expression of AQP-2, its phosphorylation, and consequent translocation from intracellular vesicles to the apical membrane of the collecting duct epithelial cells (4). Via this pathway water is passively reabsorbed from the urinary collecting ducts to cells from whence it is retrieved into the blood through AQP3 and AQP4 located on the basolateral membrane of ductal cells (5).

Seven AQPs are expressed in the kidney (6). In addition to AQP2, AQP3 and AQP4 are involved in the described AVP pathway, and AQP1 controls water reabsorption in the proximal tubule, in the descending thin limbs of Henle, and in the descending vasa recta. The remaining channels, AQP6, AQP7, and AQP11 are involved in urinary acid secretion, glycerol transport, and endoplasmic reticulum homeostasis, respectively (6).

Liver X receptor β (LXRβ) is a ligand-activated transcription factor belonging to the superfamily of nuclear hormone receptors with a key role in lipid homeostasis. It shares more than 78% sequence homology with its α isoform (LXRα). Both family members heterodimerize with the retinoid X receptor (7), and both are stimulated by the same pharmaceutical and endogenous ligands, such as oxysterols, in particular by 22-hydroxycholesterol, 27-hydroxycholesterol, 24-hydroxycholesterol, and 24,25-epoxycholesterol (8). The physiological functions of the LXRs have been revealed by studies of the phenotype of the knockout mice (9). One characteristic of LXRβ$^{-/-}$ mice is a severe pancreatic insufficiency that leads to malabsorption and resistance to weight gain (10). In addition, there are sex differences in the response to the loss of LXRβ. LXRβ$^{-/-}$ male but not female mice develop motor neuron disease as they age (11), whereas female mice undergo progressive estrogen-dependent carcinogenesis of the gallbladder (12).

Here we show an unexpected role for LXRβ, in controlling body water balance. LXRβ$^{-/-}$ mice develop central DI with a reduced number of hypothalamic vasopressin-positive neurons and decreased urinary AVP excretion in association with a mild reduction in the renal content of AQP1. These data identify LXRβ as a key regulator of body water balance both at a neurogenic and a nephrogenic level.

Results

Polyuria, Low Urine Osmolality, and Polydipsia in LXRβ$^{-/-}$ Mice. At age 12 mo, WT, LXRα$^{-/-}$, and LXRβ$^{-/-}$ mice were housed in metabolic cages for 24 h to study their water balance. During ad libitum water intake, LXRβ$^{-/-}$ mice excreted an abnormally large volume of urine per day (Fig. 1*A*) with a low osmolality indicating pathologically high urine dilution (Fig. 1*B*). This polyuria of LXRβ$^{-/-}$ mice also was associated with a 24-h water intake much higher ($P < 0.05$) than that of WT mice (Fig. 1*C*).

Author contributions: C.G., M.W., and J.-Å.G. designed research; C.G., X.K., H.S., H.-J.K., M.G., X.J., H.O., and Y.U. performed research; C.G. and M.W. analyzed data; and C.G., M.W., Y.G., and J.-Å.G. wrote the paper.

The authors declare no conflict of interest.

[1]X.K., H.S., and H.-J.K. contributed equally to this work.

[2]To whom correspondence should be addressed. E-mail: jgustafsson@uh.edu.

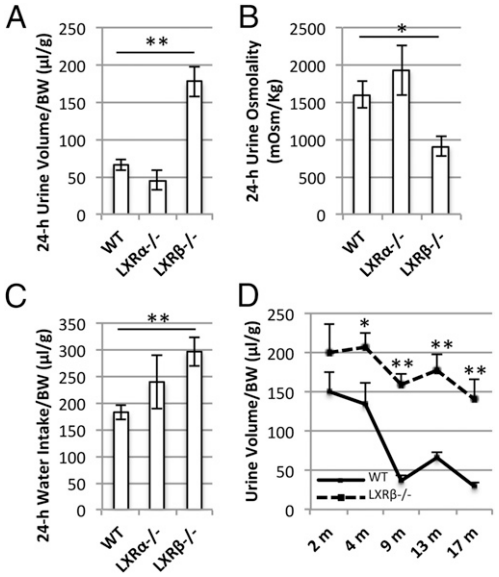

Fig. 1. Body water balance and urine osmolality in female WT (n = 10), LXRα$^{-/-}$ (n = 10), and LXRβ$^{-/-}$ (n = 10) mice. Mice were housed in metabolic cages with free access to food and water for 24 h. (*A*) The daily urine volume is significantly higher in LXRβ$^{-/-}$ mice than in WT mice. (*B*) The 24-h urine osmolality, an indication of diluted urine, is significantly lower in LXRβ$^{-/-}$ mice than in WT mice. (*C*) The 24-h water intake is higher in LXRβ$^{-/-}$ mice. (*D*) The 24-h urine volume of WT and LXRβ$^{-/-}$ mice at age 2, 4, 9, 13, and 17 mo (n = 8 each group). The onset of polyuria appears to occur at age 4 mo. Data are presented as mean ± SEM; *P < 0.05; **P < 0.001 versus WT.

To distinguish further the LXRβ$^{-/-}$ polyuria from an osmotic diuresis caused by the presence of high concentration of solutes such as glucose or urea in the fluid filtered by the kidney, a chemical analysis of the urine was performed (Table 1). The concentration of glucose, urea, and other solutes was significantly lower in the urine of LXRβ$^{-/-}$ mice than in the urine of WT mice. Furthermore in LXRβ$^{-/-}$ mice serum creatinine was in the normal range, thus excluding an intrinsic renal disease (Table 1).

LXRα$^{-/-}$ mice did not differ from WT mice in their daily urine volume or osmolality or in water intake (Fig. 1 *A*–*C*). Therefore the condition of polyuria and polydipsia, characteristics of DI (1), appeared to be specific for LXRβ$^{-/-}$ mice, and the onset occurred as early as age 4 mo (Fig. 1*D*).

Table 1. Urine and serum chemistry profile in 12-mo-old WT and LXRβ$^{-/-}$ mice

Chemistry profile	WT	LXRβ$^{-/-}$
Urine		
pH	7.2 ± 0.2	6.3 ± 0.1**
Glucose (mg/dL)	40.1 ± 4.2	23.9 ± 2.0*
Total Protein (mg/dL)	317 ± 36	55 ± 8**
Creatinine (mg/dL)	42.0 ± 3.5	18.7 ± 1.5**
Urea Nitrogen (mg/dL)	3085 ± 285	1535 ± 108**
Sodium (mmol/L)	114 ± 12	51 ± 4**
Potassium (mmol/L)	204 ± 19	122 ± 9**
Calcium (mg/dL)	14 ± 1	8 ± 1**
Magnesium (mg/dL)	55 ± 5	33 ± 2**
Phosphorus (mg/dL)	135 ± 9	86 ± 8**
Serum		
Creatinine (mg/dL)	0.38 ± 0.06	0.37 ± 0.03

Data are presented as mean ± SEM; *P < 0.05; **P < 0.001 versus WT. n = 10 per group for the urine chemistry profile, and n = 5 per group for the serum creatinine.

Partial Ability of LXRβ$^{-/-}$ Mice to Respond to Dehydration. To differentiate a primary polydipsia from other forms of DI, WT, LXRα$^{-/-}$, and LXRβ$^{-/-}$ mice were deprived of water for 24 h in metabolic cages. A significant contraction of the daily urinary volume was detectable in all three strains of mice during the dehydration period (Fig. 2*A*). Nevertheless, water-deprived LXRβ$^{-/-}$ mice had a higher urine output (P < 0.05) than dehydrated WT mice (Fig. 2*A*), excluding a primary polydipsia. During dehydration, serum and urine osmolalities were significantly increased in LXRβ$^{-/-}$ mice as well as in WT and LXRα$^{-/-}$ mice (Fig. 2 *B* and *C*). However, urine osmolality was significantly lower (P < 0.05) in the water-deprived LXRβ$^{-/-}$ mice in than in dehydrated WT mice, indicating a partially conserved ability to respond to water deprivation.

During the 24-h period of water deprivation, the observed polyuria of LXRβ$^{-/-}$ mice was associated with a body weight loss of more than 20%, significantly higher than that of WT mice (Fig. 2*D*), suggesting severe dehydration. Food intake did not differ between the three strains during dehydration (Fig. 2*E*).

Partial Response to Exogenous AVP in LXRβ$^{-/-}$ Mice. To distinguish further central from nephrogenic DI, WT and LXRβ$^{-/-}$ mice were injected i.p. with 1 µg/kg of AVP in 100 µL saline solution. Urine volume and osmolality were monitored 3 and 6 h after injection. In WT mice, there was a significant reduction in urine volume after AVP stimulation (Fig. 3*A*) with an increase in urine osmolality (Fig. 3*B*). LXRβ$^{-/-}$ mice failed to reduce the urine output but significantly increased urine osmolality after 6 h (Fig. 3*B*). This partial response of LXRβ$^{-/-}$ mice to exogenous AVP indicates a conserved renal ability to concentrate urine and a possible central pathogenesis of DI.

Reduction of AVP Expression in Neurons and Neuronal Projections in the PVN and SON of LXRβ$^{-/-}$ Mice. To determine whether there was a loss of AVP-positive neurons in LXRβ$^{-/-}$ mice, brains were immunostained with monoclonal antibody against AVP. In the

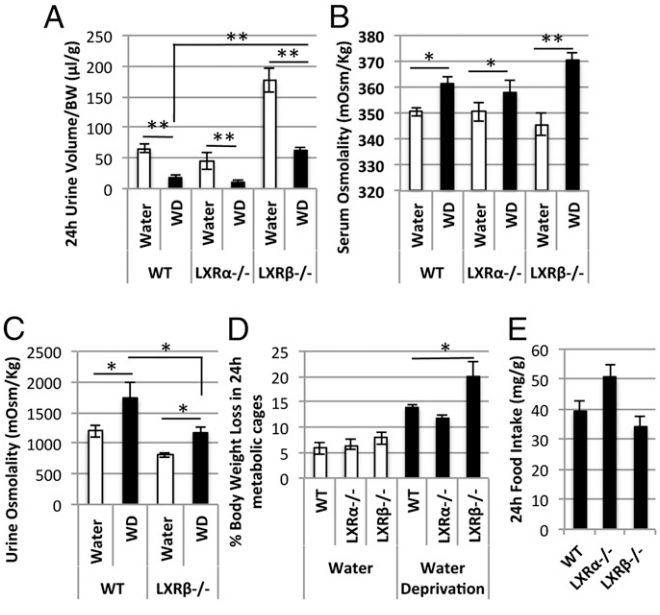

Fig. 2. Water-deprivation test in female WT (n = 10), LXRα$^{-/-}$ (n = 10), and LXRβ$^{-/-}$ (n = 10) mice. (*A*) The 24-h urine volume was significantly decreased in all three strains studied after dehydration (WD), with a parallel increase in serum osmolality (*B*). (*C*) Urine osmolality is increased in dehydrated as compared with nondehydrated LXRβ$^{-/-}$ and WT mice. (*D*) The percentage of body weight loss during water deprivation is significantly higher in LXRβ$^{-/-}$ mice than in dehydrated WT mice. (*E*) Food intake was not affected during water deprivation. Data are presented as mean ± SEM; *P < 0.05; **P < 0.001 versus WT.

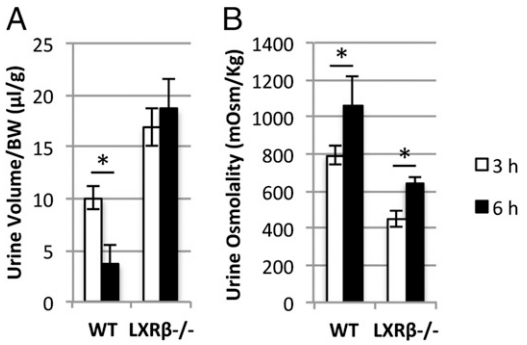

Fig. 3. Urine volume and osmolality after AVP administration. Mice were injected i.p. with AVP and then were housed in metabolic cages. Urine was collected after 3 and 6 h. (*A*) Urine volume was contracted significantly after 6 h in WT mice but not in LXRβ$^{-/-}$ mice. (*B*) Urine osmolality was increased significantly at 6 h in both WT and LXRβ$^{-/-}$ mice. Data are presented as mean ± SEM; *$P < 0.05$ versus WT.

PVN of WT mice (Fig. 4*A*) positive immunoreactivity was detected in both the cell bodies of magnocellular neurons and in their neuronal projections. In contrast, LXRβ$^{-/-}$ mice exhibited fewer vasopressin-positive neurons, and the staining of the projections was barely detectable (Fig. 4*B*). A similar loss of vasopressinergic neurons was detected in the SON of LXRβ$^{-/-}$ mice (Fig. 4*D*) as compared with WT animals (Fig. 4*C*). The number of AVP-positive neurons was counted and found to be significantly reduced in LXRβ$^{-/-}$ mice, whereas, as expected, LXRα$^{-/-}$ mice did not show any pathological AVP immunoreactivity in either the PVN or SON (Fig. 4*E*).

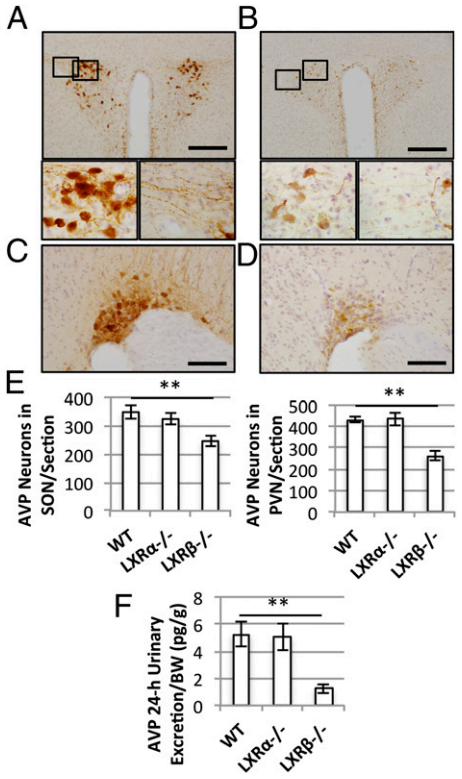

Fig. 4. Immunohistochemical detection of hypothalamic vasopressin-positive neurons. (*A*) Representative hypothalamic section of the PVN of a 12-mo-old WT mouse. (Scale bar: 100 μm.) (*Bottom*) Higher magnification of the selected areas showing AVP-positive cell bodies (*Left*) and neuronal projections (*Right*). (*B*) PVN of a 12-mo-old LXRβ$^{-/-}$ mouse. (Scale bar: 100 μm.) (*Bottom*) Higher magnification of selected areas. Reduced immunoreactivity for AVP was detected both in the magnocellular neurons (*Left*) and in their projections (*Right*). (*C* and *D*) Representative sections of SON in WT (*C*) and LXRβ$^{-/-}$ mice (*D*). (Scale bars: 50 μm.) (*E*) Numbers of AVP-positive neurons per section in SON (*Left Inset*) and PVN (*Right Inset*). Data are presented as mean ± SEM; **$P < 0.001$ versus WT. $n = 6$ in each group. (*F*) Urinary AVP excretion in 24 h. The urinary AVP content was reduced significantly in LXRβ$^{-/-}$ mice compared with WT animals. Data are presented as mean ± SEM; **$P < 0.001$ versus WT. $n = 6$ in each group.

Reduced 24-h Urinary Excretion of AVP in LXRβ$^{-/-}$ Mice. To confirm the neuronal origin of DI in LXRβ$^{-/-}$ mice, urinary AVP excretion was measured as an indicator of central AVP release, as previously described (13). The 24-h AVP excretion (Fig. 4*F*) was significantly ($P < 0.001$) lower in LXRβ$^{-/-}$ mice than in WT mice, whereas no differences were detected between WT and LXRα$^{-/-}$ mice, confirming that LXRβ$^{-/-}$ mice are specifically affected by a central DI.

LXRβ Is Expressed in the Magnocellular Neurons of the SON and PVN of the Hypothalamus. To investigate the possible influence of LXRβ on the loss of AVP neurons in LXRβ$^{-/-}$ mice, LXRβ localization and expression in the hypothalamus was studied with immunohistochemistry. In WT mice, positive immunoreactivity for LXRβ was detected in the nuclei of the magnocellular neurons in both the PVN (Fig. 5*A*) and SON (Fig. 5*B*) of the hypothalamus. There was also some cytoplasmic staining in the SON neurons.

Reduced AQP1 Immunoreactivity in the Kidney of LXRβ$^{-/-}$ Mice. Although there was a clear central etiology of the DI in LXRβ$^{-/-}$ mice, the response of the kidney to exogenous AVP was not complete. We therefore examined the kidney more closely. Given that LXRβ is a pivotal regulator of AQP1 in the pancreatic ductal epithelial cells (10), the expression and localization of AQP1 in the kidney was studied. As expected, immunoreactivity for AQP1 in the kidney of WT mice was evident in the proximal tubule (Fig. 6*A*), in the descending thin limb of the loop of Henle (Fig. 6*B*), and in the vasa recta (Fig. 6*C*). In LXRβ$^{-/-}$ mice staining was weaker in the proximal tubule and in the thin limb of the loop of Henle (Fig. 6 *A* and *B*) but not in the vasa recta (Fig. 6*C*).

Increased Urine Osmolality After 7 d of GW3965 Treatment. To determine whether activation of LXRβ could affect body water balance, WT mice were treated with the LXR agonist GW3965 for 7 d and then were housed in metabolic cages for 24 h with free access to water and food. Although no significant differences were detected in water intake, urine volume, or serum osmolality, the urine osmolality was significantly increased in GW3965-treated mice (Table 2).

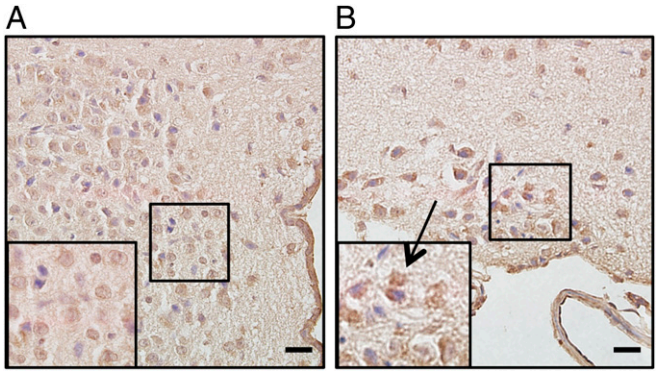

Fig. 5. Immunohistochemical study of the expression of LXRβ in the hypothalamus of 8-mo-old WT female mice. (*A*) A representative section of the PVN. Positive immunoreactivity for LXRβ is detectable in the magnocellular neurons. (*B*) Positive staining for LXRβ is shown in the SON (arrow). *Insets* show higher magnification of the selected areas. (Scale bars: 20 μm.)

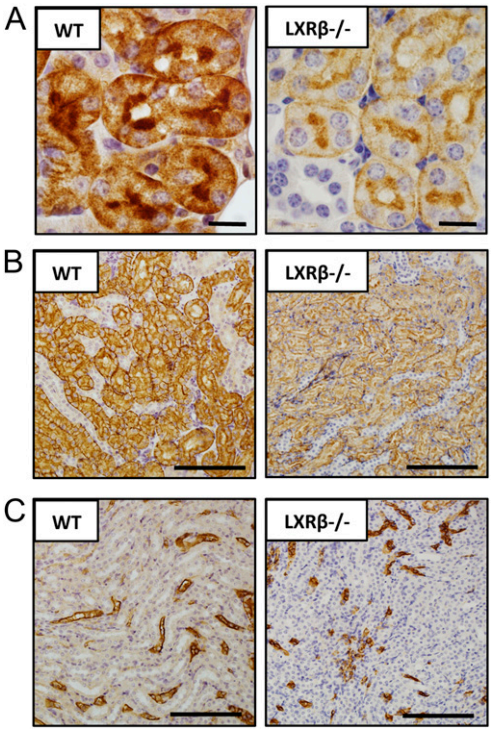

Fig. 6. Immunohistochemical study of AQP-1 expression in the kidney of 12-mo-old WT and LXRβ$^{-/-}$ female mice. In WT mice AQP-1 immunoreactivity was detectable in the renal proximal tubule (*A*), in the descending thin limb of Henle (*B*), and in the vasa recta (*C*). In LXRβ$^{-/-}$ mice the positive staining was evident with a markedly lower reactivity in the proximal tubule (*A*) and in the descending thin limb of Henle (*B*) but not in the vasa recta (*C*). (Scale bars: 10 μm in *A*; 100 μm in *B* and *C*.)

Discussion

In this study we analyzed LXRα$^{-/-}$, LXRβ$^{-/-}$, and WT mice to delineate the role of LXRs in the regulation of water balance both in the brain and in the kidney. The study revealed that by age 4 mo, LXRβ$^{-/-}$ but not LXRα$^{-/-}$ mice are affected by DI, a condition characterized by a progressive polyuria with excretion of abnormally highly diluted urine associated with high water intake (1). Dehydration tests and administration of exogenous AVP revealed that LXRβ$^{-/-}$ mice had a conserved but reduced ability to concentrate urine.

Several animal models of DI have been generated by genetic targeting of AVP (14), its receptor AVPR2, or the water channels in the kidney. Interestingly, mice with homozygous deficiency in AVPR2 are unable to concentrate urine and die of severe dehydration within the first week after birth (15). AQP2 global knockout mice die postnatally (16), whereas mice in which AQP2 is selectively silenced in renal collecting ducts are viable but are unable to respond to water deprivation (16). In addition, mice with a truncated COOH terminus of AQP2 do not respond to desmopressin injection (17). AQP1$^{-/-}$ mice are affected by a severe polyuria with absence of any response to dehydration (18). Thus, LXRβ$^{-/-}$ mice, by concentrating urine, have a phenotype that differs from animal models of nephrogenic DI and are closer to models of central DI, especially given their reduction of AVP content both in brain and urine (14, 19).

Our immunohistochemical results reveal that LXRβ is localized in the nuclei of the magnocellular neurons of the hypothalamic SON and PVN. LXR deficiency leads to a loss of AVP production in magnocellular neurons and to a consequent impaired AVP excretion.

LXRβ is strongly expressed in the developing brain (20) and has a pivotal role in controlling the migration of cortical neurons. Newborn LXRβ$^{-/-}$ mice have a small brain with a thin cortex (20) and high levels of cholesterol in both the brain (21) and the spinal cord (11, 22); in these mice death of spinal motor neurons with age leads to motor neuron disease (11, 22). At embryonic day 14.5, neurons migrate laterally from the neuroepithelium to the SON and medially to the PVN in a precise process controlled by numerous factors such as the Notch effector Hes1 (23). Interestingly, the Notch pathway appears to be under the control of LXRs in bone marrow stromal cells (24). Based on these multiple functions of LXRβ, several hypotheses can be formulated to explain the LXRβ-related loss of AVP in magnocellular neurons, namely, cholesterol-related neurodegeneration; a developmental abnormality involved in neuronal migration; or transcriptional control by LXRβ of the AVP promoter.

Given that LXRβ regulates the expression of AQP1 in the pancreas (10), the expression of this water channel was studied in the kidney. Immunohistochemistry showed a reduction of AQP1 in the proximal tubule and in the thin limb of Henle, and this reduction could contribute on the one hand to polyuria and on the other to the incomplete response of LXRβ$^{-/-}$ mice to both water deprivation and exogenous AVP.

Treatment of WT mice with an LXR agonist (GW3965) leads to an increase in 24-h urine osmolality during free water access. This decrease could be caused both by a central effect on AVP production/secretion and by stimulation of AQP1 transcription in the kidney.

Interestingly, in neurons AQP1 is localized in synaptic vesicles (25) as well as in the dense core secretory granules of the pituitary where it regulates vesicular swelling during exocytosis (26). A lack of AQP1 in neuronal secretory vesicles in LXRβ$^{-/-}$ mice would be expected to affect the stability of AVP-containing vesicles and in turn their exocytosis. Moreover, the lack of AVP, together with a previously reported control by both LXRs on the basal expression of renin mRNA (27), raises the possibility of a low volume/blood pressure in LXRβ$^{-/-}$ mice. More studies will be needed to elucidate the interplay between LXRβ, AQPs, and AVP in the control of both water homeostasis and brain plasticity.

In conclusion, our results have clarified a specific role for LXRβ in regulating body water balance both at a central and a nephrogenic level, and LXRβ thus appears to be a good target candidate for treating disorders of water homeostasis. In addition, because the etiology is unknown in 30–50% of patients with

Table 2. Water balance in WT vehicle- and GW3965-treated mice

	WT vehicle	WT GW3965
Body weight (g)	30.1 ± 1.7	30.2 ± 0.7
Food intake/body weight (mg/g)	32.96 ± 1.08	41.9 ± 0.75
Water intake/body weight (mL/g)	0.1 ± 0.1	0.1 ± 0.1
24-h urine volume/body weight (μl/g)	34.4 ± 9.8	34.9 ± 9.3
24-h urine osmolality (mOsm/kg)	1563 ± 95	1826 ± 74*
Serum osmolality (mOsm/kg)	353.3 ± 6.1	343.1 ± 3.7

Data are presented as mean ± SEM; *$P < 0.05$ versus vehicle.

central DI (28), genetic analysis of these patients for mutations in LXR seems warranted.

Materials and Methods

Animals. Male and female WT LXR$\alpha^{-/-}$ and LXR$\beta^{-/-}$ mice were generated as previously described (29). Mice were back crossed onto a C57BL/6 background for 10 generations. Animals were housed on a 12-h light/dark cycle under controlled temperature (20–22 °C) and humidity (50–65%) in the Animal Care Operations facility of the University of Houston.

Experiments were approved by the local ethical committee for animal experiments, and the guidelines for the care and use of laboratory animals were followed.

Metabolic Cage Studies. Mice were housed in single-mouse metabolic cages (3600M021; Tecniplast) to collect urine over a 24-h period, first with free access to water and food and then under water deprivation. Mice were trained to the metabolic cages 1 wk before the experiments. Body weight, food intake, and water consumption were monitored.

Urine and Serum Analysis. Urine and serum osmolality were measured using a freezing-point depression osmometer (Micro-Osmometer 3300, Advanced Instruments, Inc.). Urine and serum chemistry analyses were performed by the Methodist Hospital Core Laboratory in Houston, TX.

AVP Treatment. Female WT and LXR$\beta^{-/-}$ mice were injected i.p. with 1 μg/kg of AVP (V0377; Sigma-Aldrich) in 100 μL saline solution. Basal urines were collected by bladder massage. Animals then were housed in metabolic cages, and urine volume and osmolality were monitored after 3 and 6 h.

Tissue Processing. Mice were killed with CO_2 asphyxiation and then were perfused transcardially with PBS followed by 4% (wt/vol) paraformaldehyde in PBS. Brains and kidneys were removed and postfixed with 4% paraformaldehyde in PBS for 24 h at 4 °C. The tissues then were cryoprotected in 30% sucrose in PBS for 48 h at 4 °C. Fixed brains were cut at 30-μm thickness with a cryostat at −20 °C. The location of the SON and the PVN was determined as previously described (30). Kidneys were paraffin embedded and then cut at 4-μm thickness.

Immunohistochemistry. The sections were incubated in PBS containing 2% hydrogen peroxide for 60 min to block endogenous peroxidase activity. They then were rinsed twice with PBS and incubated in PBS containing 1% BSA to block nonspecific staining. The floating sections were incubated either with a primary rabbit anti-AVP antibody (T-4562; Bachem Americas, Inc.) at a dilution of 1:1,000 or with a goat anti-LXRβ antibody (10) at a dilution of 1:500 in PBS containing 1% BSA and 0.1% Nonidet P-40 for 24 h at 4 °C. After washing for 20 min in PBS containing 0.1% Nonidet P-40, the sections were incubated for 1 h with a specific biotinylated secondary antibody solution (1:200) and finally with an avidin-biotin peroxidase complex (Vectastain ABC kit; Vector Laboratories, Inc.) for 1 h. Peroxidase in the sections was visualized with diaminobenzidine for 40 s Sections were mounted onto slides, air dried, counterstained with hematoxylin, dehydrated in 100% ethanol, cleared using xylene, and then coverslipped and examined under a light microscope. The presence of a dark-brown label that appeared in cytoplasm was judged to indicate AVP-like immunoreactivity-positive cells, and the numbers of positive cells in the SON and PVN were counted separately.

Kidney sections were dewaxed in xylene and rehydrated through graded ethanol. Antigens were retrieved using a PT module for 10 min at 97 °C (A80410200; Thermo Scientific). Immunohistochemistry was performed with the aid of a Lab Vision Autostainer 360 (Thermo Scientific) according to the manufacturer´s instructions. Sections were counterstained with Mayer´s hematoxylin, dehydrated through a graded ethanol series and xylene, and were mounted.

Measurement of AVP in 24-h Urine. AVP concentrations in the urine were determined with a vasopressin RIA kit according to manufacturer´s instructions (Mitsubishi-Kagaku).

LXR Agonist Treatment. Ten male C57B16/J mice (8 mo old) were treated with LXR agonist GW3965 (2474; Tocris) (10 mg/kg body weight) dissolved in PBS/DMSO (3/1 vol/vol) given daily by oral gavage for 7 d. Ten WT mice were given vehicle only for 7 d.

Statistical Analyses. Data are expressed as mean ± SEM, and the Student's *t* test was used to analyze individual differences. A value of $P < 0.05$ was considered to be statistically significant. Statistical analysis was performed with the aid of SPSS statistical software (v. 19.0 for Mac).

ACKNOWLEDGMENTS. We thank Christopher Brooks, Kaberi Das, and Laurie Minze for invaluable technical support. This work was supported by grants from the Robert A. Welch Foundation, the Swedish Science Fund, and the Texas Emerging Technology Fund (to J-Å.G.). Support for this project also was provided by Ministry of Science and Technology Grant 2012CB517504 and Natural Science Foundation Grant 81030003/30821001 (to Y.G.) and by Grant-in-Aid for Scientific Research 21591964 from the Ministry of Education, Culture, Sports, Science and Technology, Japan (to H.O.).

1. Babey M, Kopp P, Robertson GL (2011) Familial forms of diabetes insipidus: Clinical and molecular characteristics. *Nat Rev Endocrinol* 5;7(12):701–714.
2. Robertson GL (2001) Antidiuretic hormone. Normal and disordered function. *Endocrinol Metab Clin North Am* 30:671–694, vii.
3. Robertson GL (1980) Control of the posterior pituitary and antidiuretic hormone secretion. *Contrib Nephrol* 21:33–40.
4. Deen PM, et al. (1994) Requirement of human renal water channel aquaporin-2 for vasopressin-dependent concentration of urine. *Science* 264:92–95.
5. Ishibashi K, et al. (1997) Immunolocalization and effect of dehydration on AQP3, a basolateral water channel of kidney collecting ducts. *Am J Physiol* 272:F235–F241.
6. Noda Y, Sohara E, Ohta E, Sasaki S (2010) Aquaporins in kidney pathophysiology. *Nat Rev Nephrol* 6:168–178.
7. Apfel R, et al. (1994) A novel orphan receptor specific for a subset of thyroid hormone-responsive elements and its interaction with the retinoid/thyroid hormone receptor subfamily. *Mol Cell Biol* 14:7025–7035.
8. Janowski BA, et al. (1999) Structural requirements of ligands for the oxysterol liver X receptors LXRalpha and LXRbeta. *Proc Natl Acad Sci USA* 96:266–271.
9. Gabbi C, Warner M, Gustafsson JA (2009) Minireview: Liver X receptor beta: Emerging roles in physiology and diseases. *Mol Endocrinol* 23:129–136.
10. Gabbi C, et al. (2008) Pancreatic exocrine insufficiency in LXRbeta-/- mice is associated with a reduction in aquaporin-1 expression. *Proc Natl Acad Sci USA* 105:15052–15057.
11. Andersson S, Gustafsson N, Warner M, Gustafsson JA (2005) Inactivation of liver X receptor beta leads to adult-onset motor neuron degeneration in male mice. *Proc Natl Acad Sci USA* 102:3857–3862.
12. Gabbi C, et al. (2010) Estrogen-dependent gallbladder carcinogenesis in LXRbeta-/- female mice. *Proc Natl Acad Sci USA* 107:14763–14768.
13. Morishita T, et al. (2005) Nephrogenic diabetes insipidus in mice lacking all nitric oxide synthase isoforms. *Proc Natl Acad Sci USA* 102:10616–10621.
14. Grant FD (2000) Genetic models of vasopressin deficiency. *Exp Physiol* 85(Spec No):203S–209S.
15. Yun J, et al. (2000) Generation and phenotype of mice harboring a nonsense mutation in the V2 vasopressin receptor gene. *J Clin Invest* 106:1361–1371.
16. Rojek A, Füchtbauer EM, Kwon TH, Frøkiaer J, Nielsen S (2006) Severe urinary concentrating defect in renal collecting duct-selective AQP2 conditional-knockout mice. *Proc Natl Acad Sci USA* 103:6037–6042.
17. Shi PP, et al. (2007) Nephrogenic diabetes insipidus in mice caused by deleting COOH-terminal tail of aquaporin-2. *Am J Physiol Renal Physiol* 292:F1334–F1344.
18. Ma T, et al. (1998) Severely impaired urinary concentrating ability in transgenic mice lacking aquaporin-1 water channels. *J Biol Chem* 273:4296–4299.
19. Russell TA, et al. (2003) A murine model of autosomal dominant neurohypophyseal diabetes insipidus reveals progressive loss of vasopressin-producing neurons. *J Clin Invest* 112:1697–1706.
20. Fan X, Kim HJ, Bouton D, Warner M, Gustafsson JA (2008) Expression of liver X receptor beta is essential for formation of superficial cortical layers and migration of later-born neurons. *Proc Natl Acad Sci USA* 105:13445–13450.
21. Kim HJ, et al. (2008) Liver X receptor beta (LXRbeta): A link between beta-sitosterol and amyotrophic lateral sclerosis-Parkinson's dementia. *Proc Natl Acad Sci USA* 105:2094–2099.
22. Bigini P, et al. (2010) Neuropathologic and biochemical changes during disease progression in liver X receptor beta-/- mice, a model of adult neuron disease. *J Neuropathol Exp Neurol* 69:593–605.
23. Aujla PK, Bora A, Monahan P, Sweedler JV, Raetzman LT (2011) The Notch effector gene Hes1 regulates migration of hypothalamic neurons, neuropeptide content and axon targeting to the pituitary. *Dev Biol* 353:61–71.
24. Kim WK, et al. (2010) Osteogenic oxysterol, 20(S)-hydroxycholesterol, induces notch target gene expression in bone marrow stromal cells. *J Bone Miner Res* 25:782–795.
25. Jeremic A, Cho WJ, Jena BP (2005) Involvement of water channels in synaptic vesicle swelling. *Exp Biol Med (Maywood)* 230:674–680.
26. Arnaoutova I, et al. (2008) Aquaporin 1 is important for maintaining secretory granule biogenesis in endocrine cells. *Mol Endocrinol* 22:1924–1934.
27. Morello F, et al. (2005) Liver X receptors alpha and beta regulate renin expression in vivo. *J Clin Invest* 115:1913–1922.
28. Maghnie M, et al. (2000) Central diabetes insipidus in children and young adults. *N Engl J Med* 343:998–1007.
29. Alberti S, et al. (2001) Hepatic cholesterol metabolism and resistance to dietary cholesterol in LXRbeta-deficient mice. *J Clin Invest* 107:565–573.
30. Paxinos G, Franklin KBJ (2001) *The Mouse Brain in Stereotaxic Coordinates.* (Academic Press, San Diego, CA) 2nd Ed.